



Published in final edited form as:

ACS Chem Neurosci. 2010 February 17; 1(2): 95–103. doi:10.1021/cn900024r.

Effectiveness of Novel Borane-Phosphine Complexes In Inhibiting Cell Death Depends on the Source of Superoxide Production Induced by Blockade of Mitochondrial Electron Transport

Emily A. Seidler¹, Christopher J. Lieven¹, Alex F. Thompson¹, and Leonard A. Levin^{1,2,*}

¹Department of Ophthalmology and Visual Sciences, University of Wisconsin School of Medicine and Public Health

²Department of Ophthalmology, University of Montreal

Abstract

Central neurons undergo cell death after axotomy. One of the signaling pathways for this process is oxidative modification of one or more critical sulfhydryls in association with superoxide generation within mitochondria. Agents that reduce oxidized sulfhydryls are neuroprotective of axotomized retinal ganglion cells, and we hypothesized that this occurs via reversal of the effects of mitochondrial-produced superoxide. To study this, we measured the ability of the novel borane-phosphine complex drugs bis(3-propionic acid methyl ester)phenylphosphine borane complex (PB1) and (3-propionic acid methyl ester)diphenylphosphine borane complex (PB2) to inhibit the death of neuron-like RGC-5 cells induced by perturbation of the mitochondrial electron transport chain. We found that borane-phosphine complexes prevent neuronal cell death from superoxide produced by the redox-cycling agent menadione and the complex III inhibitor antimycin A, which produce superoxide towards the cytoplasm and matrix, but not the complex I inhibitor rotenone, which produces superoxide in the matrix alone. The ability of these disulfide reductants to prevent cell death may be predicted by the topology of superoxide production with respect to the mitochondrial matrix and extramitochondrial space.

Keywords

Superoxide; mitochondria; axonal injury; retinal ganglion cells; sulfhydryl modification

Introduction

Retinal ganglion cells (RGCs) are archetypal central neurons that undergo apoptosis after axonal injury (1,2). RGCs have an optimal redox state for survival after axotomy, in that a reduced redox state is associated with increased survival, compared to neutral or more oxidized conditions (3,4). The disulfide-reducing agent tris(2-carboxyethyl)phosphine (TCEP) dramatically increases survival of cultured retinal ganglion cells after axotomy *in vitro* (4) and *in vivo* (5), even in the absence of exogenous neurotrophic factors. Similar but quantitatively lower levels of neuroprotection are seen with dithiothreitol, which also reduces disulfides (4). Together, these findings are consistent with a mechanism whereby oxidation of one or more critical sulfhydryls is a signaling step for the induction of apoptosis in RGCs after axotomy. One of the possible sources of oxidative species is the generation of superoxide anion after

*Corresponding Author: Leonard A. Levin, M.D., Ph.D., Department of Ophthalmology and Visual Sciences, University of Wisconsin Medical School, 600 Highland Avenue, Madison, WI 53792, (608) 265-6546.

axonal injury to the retinal ganglion cell (6), probably of mitochondrial origin (6,7). Supporting this, menadione-induced mitochondrial superoxide causes changes in the redox status of neuronal sulfhydryls (8).

Given that (1) oxidative modification of one or more critical sulfhydryls on signaling proteins is part of the signal pathway for neuronal death; (2) superoxide is generated in mitochondria after axotomy; and (3) mitochondria induce apoptosis by release of cytochrome c and other apoptosis inducing factors, we hypothesized that reduction of oxidatively modified sulfhydryls by TCEP and related molecules could be the mechanism by which this and similar drugs are neuroprotective. To study this further, we developed novel forms of disulfide reducing agents, with molecular features that increased penetration of cell membranes, increased retention within the cell, and protected the drugs from degradation by oxidation (9). This class of drugs is neuroprotective of RGCs *in vitro*, being active at picomolar to nanomolar concentrations (9).

To test the hypothesis that the mechanism of action for this class of drugs is via reversal of the effects of oxidative species generated in mitochondria, we measured their ability to inhibit the death of neuron-like RGC-5 cells induced by perturbation of the mitochondrial electron transport chain (METC). We found that the ability to prevent cell death due to mitochondrial disruption was not due to direct scavenging of superoxide within the cell, and was specific to the site of superoxide generation with respect to the mitochondrial matrix.

Results and Discussion

Dose-dependent toxicity of mitochondrial electron transport chain inhibition and reactive oxygen induction in RGC-5 cells

RGC-5 cells plated in 96-well plates were treated for 24 hours with the redox cycling agent menadione, the complex I inhibitor rotenone, or the complex III inhibitor antimycin A, at final concentrations ranging from 100 nM to 31.6 μ M (menadione) or 1 μ M to 316 μ M (rotenone, antimycin A). There was a dose-response relationship between these METC-active drugs and RGC-5 viability (Figure 1).

To assess neuroprotection with PB1 and PB2 compounds, the initial dose-response curves were used to choose a single concentration of each METC-active drug that would achieve 50-70% cell death (menadione and rotenone at 3.16 μ M; antimycin A at 1 μ M). RGC-5 cells were then co-incubated with the METC-active drugs and a range of concentrations of the borane-phosphines PB1 or PB2 for 24 hours, followed by assessment of cell viability by calcein/propidium iodide assay. TCEP (100 μ M) served as a positive control.

PB1 and PB2 showed significant rescue of RGC-5 cells from death induced by METC-active drugs menadione, rotenone, and antimycin A. PB1 was highly neuroprotective when given to RGC-5 cells at a final concentration of 100 μ M against menadione ($83 \pm 5\%$ vs. $34 \pm 4\%$; $p < 0.0001$) and against antimycin A ($74 \pm 4\%$ vs. $34 \pm 2\%$; $p < 0.0001$). PB1 rescue from rotenone-induced oxidative stress was significant, but substantially less than for the other METC-active drugs ($36 \pm 3\%$ vs. $25 \pm 3\%$; $p = 0.01$) (Figure 2). PB2 was highly neuroprotective at a final concentration of 1 μ M against menadione ($95 \pm 5\%$ vs. $34 \pm 4\%$; $p < 0.0001$) and antimycin A ($68 \pm 3\%$ vs. $34 \pm 2\%$; $p < 0.0001$). As with PB1, PB2 showed significant but substantially lower protection from rotenone ($34 \pm 2\%$ vs. $25 \pm 3\%$; $p = 0.03$) (Figure 3). At higher concentrations, PB1 and PB2 show little or no rescue of RGC-5 cells, most likely due to toxicity.

PB1 and PB2 show significantly more rescue than tris(2-carboxyethyl)phosphine at the same or lower dose

We used PB1 and PB2, members of the borane-protected phosphine class of reducing agents, because they are cell-permeable analogs of TCEP with consequently greater rescue of primary RGCs (9). We compared the ability of TCEP to rescue RGC-5 cells with that of PB1 and PB2. PB1 and PB2 showed significantly more rescue than TCEP in RGC-5 cells co-treated with superoxide-generating compounds (Figure 4). PB1 and PB2 rescued cells to a level indistinguishable from control (menadione, $p = 0.45, 0.70$; antimycin A, $p = 0.79, 0.82$), and significantly higher than TCEP for the same treatment for 5 of the 6 comparisons ($p < 0.05$).

PB1 and PB2 do not scavenge superoxide

METC inhibition causes a significant production of mitochondrial superoxide as a result of reduced complexes leaking electrons to free molecular oxygen. The decrease in cell death by PB1 and PB2 following METC inhibition could therefore result either from a direct interaction between the borane-phosphine complex and superoxide, or chemical reduction of oxidized thiols. To distinguish these two possibilities, we assessed the ability of PB1, PB2, or the unprotected phosphine-based reducing agent TCEP to scavenge superoxide in a cell-free assay. Dihydroethidium (HET) was used to measure superoxide levels in the presence of xanthine and xanthine oxidase, a superoxide-generating system, in the presence and absence of the phosphines. Superoxide dismutase (SOD) was used as a positive control. While SOD produced the expected dose-dependent reduction of HET fluorescence ($80527 \pm 535, 75117 \pm 546, 57238 \pm 428, \text{ and } 26321 \pm 671$ for 0, 1, 10, and 100 U/ml, respectively, in arbitrary fluorescence units; $p = 0.002, p < 0.0001, \text{ and } p < 0.0001$ vs control, respectively), PB1 and PB2 produced a minimal reduction in superoxide levels and only at the lower concentrations (77116 ± 501 and 74530 ± 180 for 1 μM and 10 μM PB1, respectively, and 77342 ± 892 for 1 μM PB2; $p = 0.01, 0.004, \text{ and } 0.05$, respectively) (Figure 5). To rule out the possibility that the protective borane group could inhibit superoxide scavenging in cell-free conditions, the compounds were stripped of this group by incubation in the presence of DABCO, followed by measurement of superoxide as above. PB1 and PB2 deprotected in this manner still did not significantly scavenge superoxide, with similar lack of activity to TCEP, a phosphine which does not contain borane (Figure 5). These results, and the lack of a dose-dependent reduction in superoxide levels, imply that the borane-phosphine compounds PB1 and PB2 do not scavenge superoxide in a cell-free system.

It is possible that PB1 and PB2 undergo reactions within the cell (Figure 6A) that would make them able to scavenge superoxide. In order to rule this out, RGC-5 cells were treated with menadione, following which intracellular superoxide was measured with HET. Menadione (17.8 μM) caused a significant increase in intracellular superoxide levels at two hours over background compared to untreated cells (12567 ± 766 vs. -360 ± 141 ; $p < 0.0001$) (Figure 6B), consistent with its action as a redox cycling agent. Incubation of cells with PEG-SOD immediately prior to menadione significantly reduced the menadione-induced increase in HET fluorescence (3218 ± 603 ; $p < 0.0001$). Treatment of the cells with PB1 or PB2 did not result in a substantial decrease in the rate of HET oxidation ($p = \text{n.s.}$ for all treatments compared to menadione alone). PB2 actually induced a noticeable, but not significant, rise in HET fluorescence at 100 μM . Given that we observe toxicity in the cells at this concentration, this increase is not altogether surprising. Together, these results imply that PB1 and PB2 are not significant scavengers of superoxide.

Discussion

These data demonstrate that disulfide-reducing borane-phosphine complexes prevent neuronal cell death from superoxide produced by the redox-cycling agent menadione and the complex

III inhibitor antimycin A but not the complex I inhibitor rotenone. The rescue shown by the borane-phosphine complexes PB1 and PB2 against METC dysfunction in this study was substantial and significant, and not due to a direct scavenging of superoxide. These findings suggest that the topology for the chemical reduction of oxidized sulfhydryls is external to the mitochondrial matrix.

The choice of experimental paradigm influences the assessment of topology of mitochondrial superoxide production (Table). There is a general consensus that rotenone inhibition of complex I generates superoxide via increased leakage of electrons being transferred to the ubiquinone binding site of NADH dehydrogenase. The latter is physically located inside the matrix, explaining the consistent detection of 90-100% of superoxide at that location. On the other hand, there are conflicting data regarding the directionality of superoxide production via electron leakage from complex III after inhibition with antimycin A, although it is generally believed to originate from binding to the Q_i site of the complex. The widely accepted paradigm for many years, drawn from research with submitochondrial particles (SMPs), was of superoxide release into the matrix space (10). This belief shifted towards release into the intermembrane space, based on studies of whole mitochondria, use of alternative detection methods for superoxide and its dismutation byproducts, and improved understanding of the physical location of the subunits of complex III (11). Continued research has failed to definitively answer the question of what proportion of superoxide is produced towards each side of the membrane (Table) or how superoxide might translocate from the outer face of the membrane into the matrix after inhibition with antimycin A. Overall, the accumulated data is most consistent with superoxide release towards both side of the inner membrane after inhibition with antimycin A.

The literature on the topology of superoxide production after menadione treatment is limited, but shows a similar diversity of findings. Xu and Arriaga (12) measured superoxide production directed primarily towards the matrix, while Meany *et al*(13) measured generation exclusively into the intermembrane space. Both groups used highly similar methods and the same model. Differential sensitivity of the fluorescent dyes used (hydroethidium and triphenylphosphonium-hydroethidium) might lead to different sensitivities to inner- and extramitochondrial superoxide production, but most probably the findings suggests superoxide production to both sides of the inner membrane.

The pattern of neuroprotection by borane-phosphine complexes PB1 and PB2 with different mitochondrial superoxide generators therefore correlates with the topology of superoxide release. Rotenone generates superoxide exclusively into the matrix, where the bioavailability of PB1 and PB2 would be expected to be low because of the negative charge of the carboxy group after cleavage of the ester bond by nonspecific cytoplasmic esterases (Figure 7) and the negative mitochondrial membrane potential. Antimycin A and menadione lead to the production of superoxide in both the matrix and extramitochondrial spaces, with the latter being the likely site of action of these disulfide reductants. When superoxide is generated into the extramitochondrial space by redox cycling or complex III inhibition, the intracellular levels of the negatively charged phosphine ester metabolites is sufficient to reduce oxidized thiols. The intracellular charge of the phosphines therefore explains the difference between protection against complex I inhibitor-mediated neuronal death and death from complex III inhibition or redox cycling.

There are several caveats to this study. First, neuronal precursor cell line cells were used that have several phenotypic features of retinal ganglion cells, but are not the same as primary retinal ganglion cells. Second, these are *in vitro* studies of a single homogeneous cell population, and the absence of other cells that normally reside in the milieu of retinal ganglion cell within the retina could confound the results. Third, the *in vitro* conditions involves

incubation in the presence of room air and 5% CO₂ which means that cells are exposed to higher oxygen concentrations than the RGC milieu under physiological conditions in the inner retina (14). Fourth, these are mitochondrial toxins, and although their major mode of action is on the electron transport chain, we cannot exclude other nonspecific effects.

The differences between these modes of mitochondria-associated oxidation have implications for the potential therapeutic use of borane-phosphine complexes as neuroprotectants in various diseases. RGCs exhibit increased levels of superoxide dependence on complex III after axotomy (6), and are subsequently protected after acute axotomy and culture by these borane-phosphine complex compounds (9). Since complex III generates superoxide towards the cytoplasm, we would expect that the borane-phosphine complex drugs act on disulfides generated via cytoplasmic superoxide. On the other hand, diseases like Leber's hereditary optic neuropathy are due to mutations in mitochondrial DNA coding for components of complex I (15), and RGC death in this disease is likely signaled by increased levels of mitochondrially-generated superoxide (7). PB1 and PB2 would theoretically not be effective in that or related diseases, such as Leigh syndrome and Parkinson's disease. Modification of borane-protected reducing agents to achieve distribution in the mitochondrial matrix may be necessary for neuroprotection in such disorders.

Methods

Materials

RGC-5 cells were a generous gift of Neeraj Agarwal, Ph.D.. Dulbecco's modified Eagle's medium (DMEM) and penicillin-streptomycin were from Mediatech, Inc. (Manassas, VA). Fetal bovine serum (FBS) was from Gemini Bio-Products (West Sacramento, CA). Staurosporine was from Alexis Biochemicals (San Diego, CA). Diazabicyclo-2,2,2-octane (DABCO) was from Acros Organics (Geel, Belgium). Antimycin A, rotenone, menadione, xanthine, xanthine oxidase, superoxide dismutase (SOD), polyethylene glycol-conjugated superoxide dismutase (PEG-SOD), N,N-dimethylformamide, and TCEP were from Sigma-Aldrich (St. Louis, MO). Phosphate buffered saline (PBS) was from Lonza Walkersville, Inc. (Walkersville, MD). Calcein-AM and propidium iodide were from Invitrogen (Carlsbad, CA). Dihydroethidium was from Anaspec (Fremont, CA). The novel borane-protected phosphines bis(3-propionic acid methyl ester)phenylphosphine borane complex (PB1) and (3-propionic acid methyl ester)diphenylphosphine borane complex (PB2) were synthesized as previously described (9).

Cell Culture

RGC-5 cells were cultured in DMEM containing 1 g/L glucose, supplemented with 10% fetal bovine serum, 100 U/mL penicillin, and 100 µg/mL streptomycin. Cells were passaged every 48 to 72 hours when cells were approximately 60 to 75% confluent, replated at a 1:20 dilution in a 75 cm² flask in 20 ml of cell culture media and incubated at 37°C in humidified 5% CO₂. Experiments were performed in duplicate or triplicate.

Cell Treatment and Assessment of Viability

Cells were plated in 96-well plates at a density of approximately 60 cells/mm² in 50 µL of media. Approximately 24 hours after plating, cells were supplemented with an equal volume of media containing the METC-inhibitors with or without PB1 and PB2 to generate the final concentrations listed in the results. Control wells received media containing vehicle alone. Following 24 hours of treatment, media was aspirated from wells using a 25-gauge needle and cells stained with calcein-AM (10 µg/mL) and propidium iodide (1 µg/mL) in PBS for 30 minutes. Staining solution was aspirated using a 25-gauge needle and replaced with PBS. Three randomly chosen fields per well were photographed on an Axiovert 135 microscope under

epifluorescence with a Nikon D70s digital SLR camera (Nikon, Melville, NY) at a resolution of 3008×2000 pixels and an exposure time of 1.6 seconds. Live (calcein-positive) and dead (propidium iodide-positive) cells were assessed using ImageJ software. Pictures were batch analyzed using a macro containing the following actions: subtract background, threshold, erode, erode, watershed, and analyze particles between the sizes of 1000 pixels and infinity. Automated counts were periodically checked against manual counts with good agreement. The absolute amount of death in the cell culture experiments varied depending on the passage number of the RGC-5 cells and small differences between batches of cryopreserved RGC-5 cells. Because of this, each experiment was analyzed with respect to its own set of controls.

Superoxide Measurement

Cell-Free—The superoxide scavenging ability of PB1 and PB2 were assessed in a cell-free system. In the presence of superoxide, dihydroethidium (HET) is converted to an ethidium derivative that exhibits peak fluorescence in the red spectrum (excitation 480 nm, emission 586 nm). HET (1 mM) was combined with PB1, PB2, or TCEP at concentrations of 1 μ M, 10 μ M, and 100 μ M in the presence of 1 mM xanthine (X) and 0.05 U/ml xanthine oxidase (XO), a system known to generate both superoxide and hydrogen peroxide. Superoxide dismutase from bovine erythrocytes was tested as a known scavenger of superoxide at 1 U/ml, 10 U/ml, and 100 U/ml. Additionally, the borane group was removed from PB1 and PB2 by incubation at 60°C in the presence of an equimolar amount of DABCO in N,N-dimethylformamide for one hour under argon gas, followed by gradual cooling to room temperature. These de-protected compounds (dPB1 and dPB2) were also tested for scavenging ability at concentrations of 1 μ M, 10 μ M, and 100 μ M. The reaction was initiated by addition of xanthine oxidase to wells, and fluorescence was monitored every 5 minutes for 30 minutes using a 1420 Victor 2 T Multilabel Counter (excitation 485 nm, emission 580 nm). The change in HET fluorescence over 30 minutes was calculated for each well, and compared to wells receiving no scavenging compound. Experiments were performed in triplicate, and results are representative of two or more experiments.

In vitro—Superoxide levels were measured with HET in cultured cells. 24 hours after plating, RGC-5 cells in a 96-well plate were treated with 17.8 μ M menadione. PB1 or PB2 was added to treatment wells to final concentrations of 100 nM, 1 μ M, 10 μ M, or 100 μ M. Cells treated with PB1 or PB2 and menadione were compared to (1) cells treated with menadione alone; (2) cells treated with menadione and 300 U/mL PEG-SOD; (3) untreated cells. All cells were treated with 3.2 μ M HET in medium 45 minutes after treatment with menadione, PB compounds, or PEG-SOD. Fluorescence was assessed 2 hours after menadione treatment using a 1420 Victor 2 T Multilabel Counter (excitation 485 nm, emission 580 nm), with cells incubated at 37°C in humidified 5% CO₂ between readings. Conditions were performed in triplicate, and results are representative of two or more experiments.

Statistics

Viability was assessed as number of live cells/mm², and compared to untreated controls within each experiment. Means were compared using Student's unpaired *t*-test.

Acknowledgments

Funding Sources

NIH R21EY017970 and P30EY016665, Retina Research Foundation, and an unrestricted departmental grant from Research to Prevent Blindness, Inc.

References

1. Berkelaar M, Clarke DB, Wang YC, Bray GM, Aguayo AJ. Axotomy results in delayed death and apoptosis of retinal ganglion cells in adult rats. *J Neurosci* 1994;14:4368–4374. [PubMed: 8027784]
2. Garcia-Valenzuela E, Gorczyca W, Darzynkiewicz Z, Sharma SC. Apoptosis in adult retinal ganglion cells after axotomy. *J Neurobiol* 1994;25:431–438. [PubMed: 8077968]
3. Castagne V, Lefevre K, Natero R, Clarke PG, Bedker DA. An optimal redox status for the survival of axotomized ganglion cells in the developing retina. *Neuroscience* 1999;93:313–320. [PubMed: 10430495]
4. Geiger LK, Kortuem KR, Alexejun C, Levin LA. Reduced redox state allows prolonged survival of axotomized neonatal retinal ganglion cells. *Neuroscience* 2002;109:635–642. [PubMed: 11823072]
5. Swanson KI, Schlieve CR, Lieven CJ, Levin LA. Neuroprotective effect of sulfhydryl reduction in a rat optic nerve crush model. *Investigative ophthalmology & visual science* 2005;46:3737–3741. [PubMed: 16186357]
6. Lieven CJ, Schlieve CR, Hoegger MJ, Levin LA. Retinal ganglion cell axotomy induces an increase in intracellular superoxide anion. *Investigative ophthalmology & visual science* 2006;47:1477–1485. [PubMed: 16565382]
7. Hoegger MJ, Lieven CJ, Levin LA. Differential production of superoxide by neuronal mitochondria. *BMC Neurosci* 2008;9:4. [PubMed: 18182110]
8. Kloosterboer, AL.; Ribich, JR.; Levin, LA. Identification of protein targets of novel neuroprotective sulfhydryl reducing drugs; Association for Research in Vision and Ophthalmology Annual Meeting; Fort Lauderdale, FL. 2009;
9. Schlieve CR, Tam A, Nilsson BL, Lieven CJ, Raines RT, Levin LA. Synthesis and characterization of a novel class of reducing agents that are highly neuroprotective for retinal ganglion cells. *Exp Eye Res* 2006;83:1252–1259. [PubMed: 16934805]
10. Turrens JF. Superoxide production by the mitochondrial respiratory chain. *Biosci Rep* 1997;17:3–8. [PubMed: 9171915]
11. St-Pierre J, Buckingham JA, Roebuck SJ, Brand MD. Topology of superoxide production from different sites in the mitochondrial electron transport chain. *The Journal of biological chemistry* 2002;277:44784–44790. [PubMed: 12237311]
12. Xu X, Arriaga EA. Qualitative determination of superoxide release at both sides of the mitochondrial inner membrane by capillary electrophoretic analysis of the oxidation products of triphenylphosphonium hydroethidine. *Free radical biology & medicine* 2009;46:905–913. [PubMed: 19168125]
13. Meany DL, Thompson L, Arriaga EA. Simultaneously monitoring the superoxide in the mitochondrial matrix and extramitochondrial space by micellar electrokinetic chromatography with laser-induced fluorescence. *Analytical chemistry* 2007;79:4588–4594. [PubMed: 17492834]
14. Ahmed J, Braun RD, Dunn R Jr, Linsenmeier RA. Oxygen distribution in the macaque retina. *Investigative ophthalmology & visual science* 1993;34:516–521. [PubMed: 8449672]
15. Singh G, Lott MT, Wallace DC. A mitochondrial DNA mutation as a cause of Leber's hereditary optic neuropathy. *New England Journal of Medicine* 1989;320:1300–1305. [PubMed: 2566116]
16. Miwa S, Brand MD. The topology of superoxide production by complex III and glycerol 3-phosphate dehydrogenase in *Drosophila* mitochondria. *Biochimica et biophysica acta* 2005;1709:214–219. [PubMed: 16140258]
17. Muller FL, Liu Y, Van Remmen H. Complex III releases superoxide to both sides of the inner mitochondrial membrane. *The Journal of biological chemistry* 2004;279:49064–49073. [PubMed: 15317809]
18. Miwa S, St-Pierre J, Partridge L, Brand MD. Superoxide and hydrogen peroxide production by *Drosophila* mitochondria. *Free radical biology & medicine* 2003;35:938–948. [PubMed: 14556858]
19. Han D, Antunes F, Canali R, Rettori D, Cadenas E. Voltage-dependent anion channels control the release of the superoxide anion from mitochondria to cytosol. *The Journal of biological chemistry* 2003;278:5557–5563. [PubMed: 12482755]

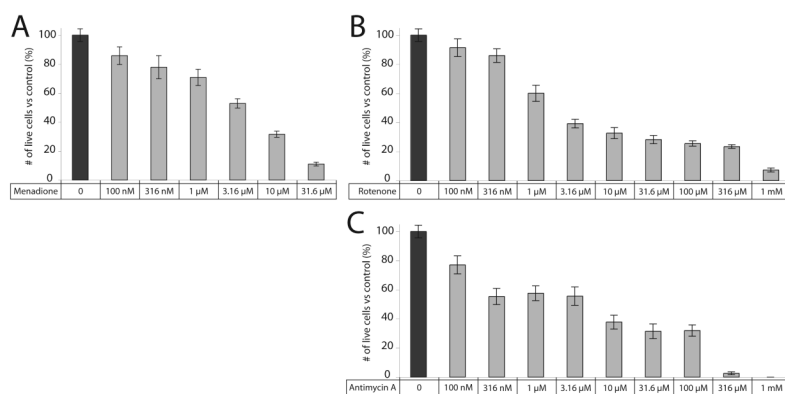


Figure 1. Cell death from METC inhibition is dose-dependent
Increasing concentrations of (A) menadione, (B) rotenone, and (C) antimycin A increase cell death in neuronal precursor RGC-5 cells.

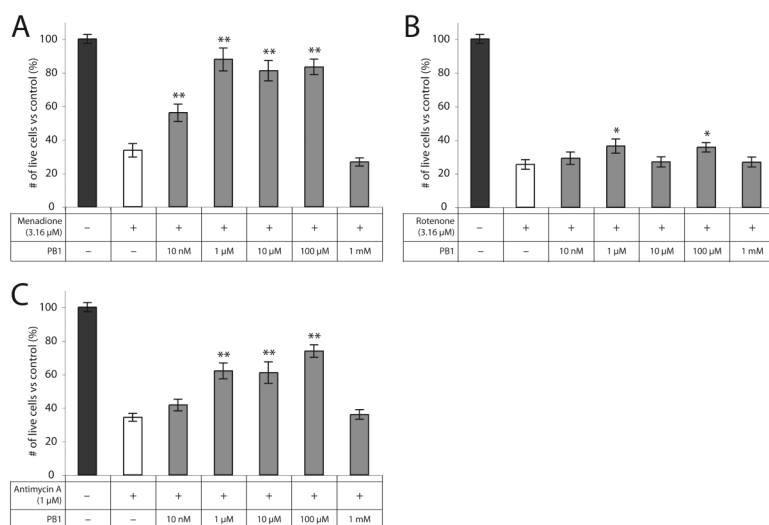


Figure 2. PB1 is protective against cell death induced by METC disruption
 PB1 is protective of RGC-5 cells against treatment with (A) menadione, (B) rotenone, and (C) antimycin A at concentrations ranging from 10 nM to 100 μ M. * ($p < 0.05$); ** ($p < 0.01$).

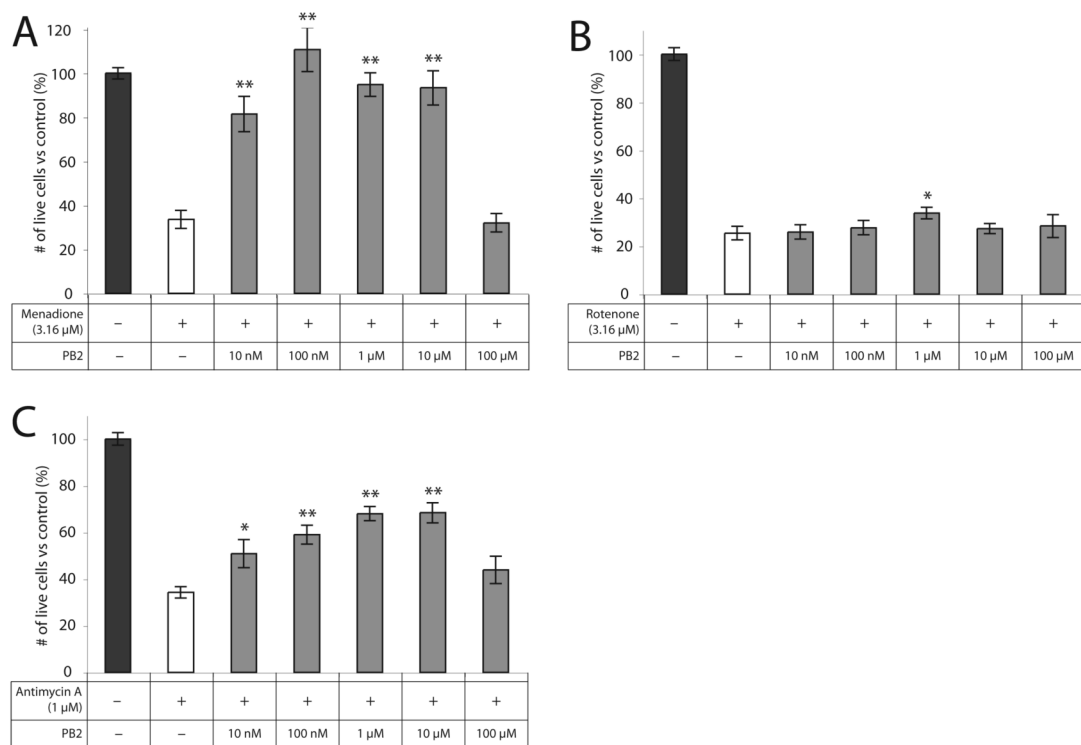


Figure 3. PB2 is protective against cell death induced by METC disruption
 PB2 is protective of RGC-5 cells against treatment with (A) menadione, (B) rotenone, and (C) antimycin A at concentrations ranging from 10 nM to 10 μ M. * ($p < 0.05$); ** ($p < 0.01$).

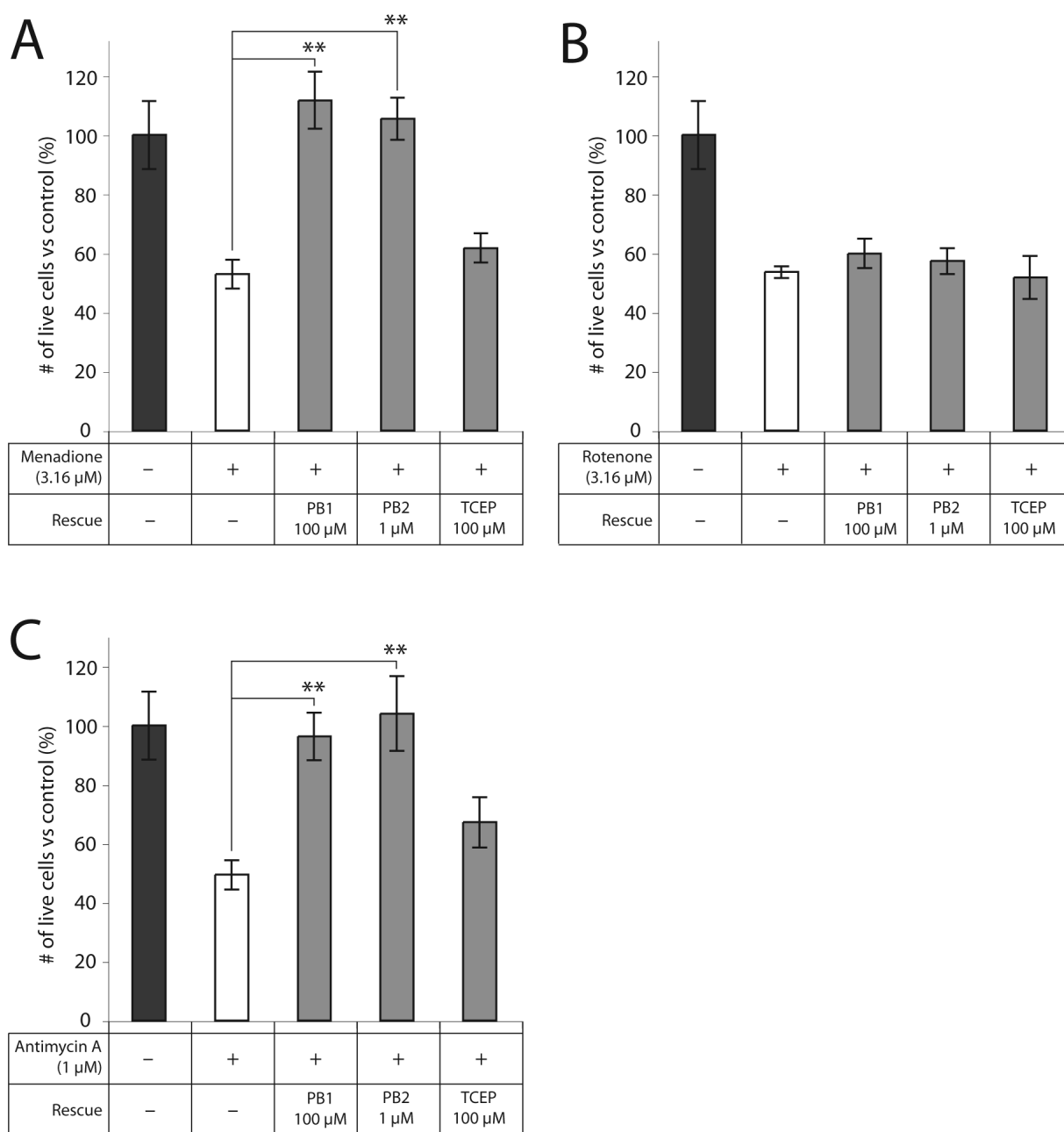


Figure 4. PB1 and PB2 exhibit greater protection than TCEP against METC disruption
 PB1 (100 μ M) and PB2 (1 μ M) significantly rescue RGC-5 cells to levels indistinguishable from control against menadione and antimycin A. TCEP does not result in significant protection against any of the METC-active compounds. ** (p<0.01).

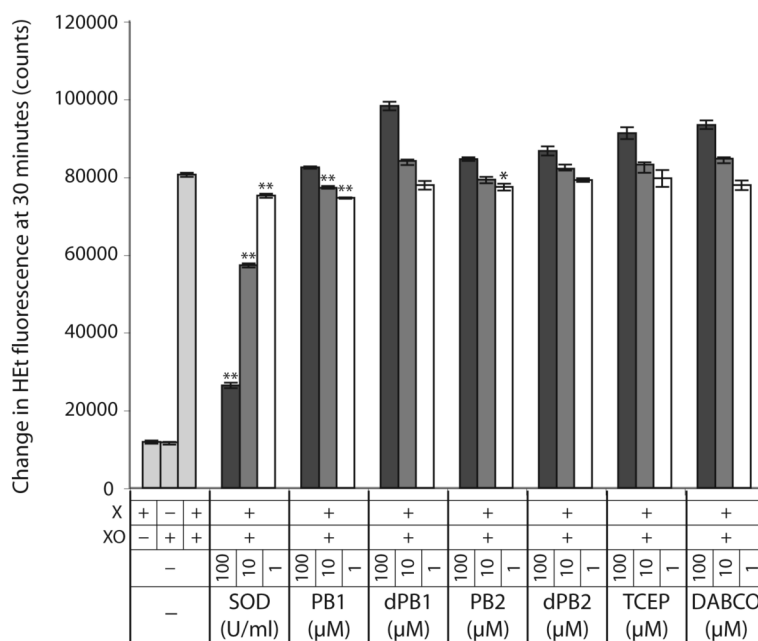


Figure 5. PB1 and PB2 do not substantially scavenge superoxide in a cell-free system
 PB1 and PB2 exhibit very low superoxide scavenging activity in a non-dose-dependent manner. Their borane-deprotected analogs (dPB1 and dPB2), as well as TCEP and the borane-deprotecting agent DABCO, do not show significant reduction in superoxide levels at any tested concentrations. * ($p < 0.05$); ** ($p < 0.01$).

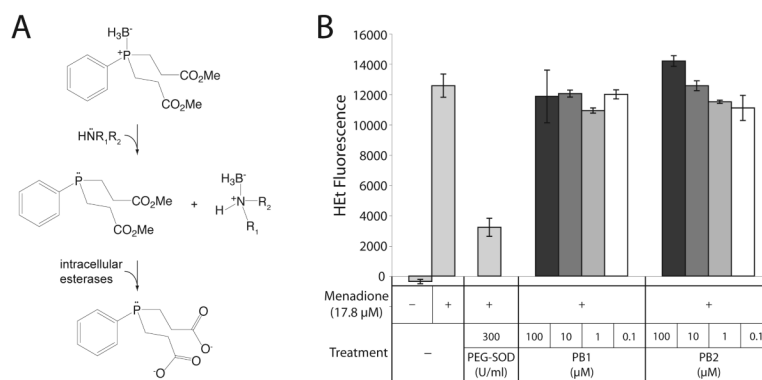


Figure 6. (A) Proposed activation of PB1 in the cell

The borane group of the borane phosphine complexes is removed by a nucleophilic attack by tissue amines. Intracellular esterases cleave the methyl ester groups, resulting in the negatively-charged, deprotected species shown. (B) PB1 and PB2 do not substantially scavenge intracellular superoxide. RGC-5 cells were incubated with menadione to generate superoxide via redox cycling, measured by oxidation of HET. PB1 and PB2 minimally affected intracellular superoxide levels. * ($p < 0.01$)

TABLE

Rotenone					
Concentration	Topology		Method	Model	Citation
	Matrix	IMS			
1 μ M - 10 μ M	100%	0%	Capillary electrophoresis of TPP-HE	143B cells (mouse)	(12)
5 μ M	~93%	~7%		Liver (mouse)	
5 μ M	~98%	~2%		Skeletal muscle (rat)	
5 μ M	> 90%	< 10%	Fluorometric detection of H ₂ O ₂ Aconitase inactivation	Drosophila	(16)
10 μ M	100%	0%	Fluorometric detection of H ₂ O ₂ Aconitase inactivation	Skeletal muscle (SOD1 -/- and WT mouse)	(17)
5 μ M	100%	0%	Fluorometric detection of H ₂ O ₂	Drosophila	(18)
10 μ M	100%	0%	Fluorometric detection of H ₂ O ₂	Heart (rat) Skeletal muscle (rat)	(11)
Menadiione					
Antimycin A					
Concentration	Topology		Method	Model	Citation
	Matrix	IMS			
	80-90%	20-10%	Capillary electrophoresis of TPP-HE	143B cells (mouse)	(12)
5 μ M	~90%	~10%		Liver (mouse)	
5 μ M	~90%	~10%		Skeletal muscle (rat)	
50 μ M	0%	100%	Capillary electrophoresis of HE	Skeletal muscle (rat)	(13)
Antimycin A					
Concentration	Topology		Method	Model	Citation
	Matrix	IMS			
	20-80%	80-20%	Capillary electrophoresis of TPP-HE	143B cells (mouse)	(12)
5 μ M	~45%	~55%		Liver (mouse)	
5 μ M	~60%	~40%		Skeletal muscle (rat)	
10 μ M	~7%	~93%	Capillary electrophoresis of HE	Skeletal muscle (rat)	(13)
	~70%	~30%	Fluorometric detection of H ₂ O ₂ Aconitase inactivation	Drosophila	(16)

Rotenone					Citation
Concentration	Topology		Method	Model	
	Matrix	IMS			
10 μ M	~50%	~50%	Fluorometric detection of H ₂ O ₂ Aconitase inactivation	Skeletal muscle (SOD1 -/- and WT mouse)	(17)
3 μ M	~65%	~35%	Fluorometric detection of H ₂ O ₂	Drosophila	(18)
1 μ g/mg protein	~30%	~70%	Fluorometric detection of O ₂ ^{-•} Fluorometric detection of H ₂ O ₂ Spin-trapping EPR	Heart (rat)	(19)
0.625 nmol/ mg protein	~20%	~80%	Fluorometric detection of H ₂ O ₂	Heart (rat)	(11)
	~40%	~60%			
2 μ M	100%	0%	Adrenochrome formation Ferricytochrome c reduction	Skeletal muscle (rat) Submitochondrial particles from heart and lung (bovine)	(10) (review)